Breast Cancer: Targets and Therapy

Dovepress
Taylor & Francis Group

Open Access Full Text Article

ORIGINAL RESEARCH

ADPB Sensitivity in Breast Cancer is Correlated with LAT1 Expression: An in vitro Study of a Novel Theranostic Candidate

Kharisma Perdani Kusumahstuti[1–3,*], Holis Abdul Holik[4,*], Muhammad Hasan Bashari[5,*], Arifudin Achmad[2,3,*], Shaharum Shamsuddin[6,*], Achmad Hussein Sundawa Kartamihardja[2,3,*]

[1]Doctoral Study Program, Faculty of Medicine, Universitas Padjadjaran, Bandung, Jawa Barat, Indonesia; [2]Department of Nuclear Medicine, Faculty of Medicine, Universitas Padjadjaran, Bandung, Jawa Barat, Indonesia; [3]Department of Nuclear Medicine and Theranostic Molekuler, Hasan Sadikin Hospital, Bandung, Jawa Barat, Indonesia; [4]Department of Pharmaceutical Analysis & Medicinal Chemistry, Faculty of Pharmacy Universitas Padjadjaran, Bandung, Jawa Barat, Indonesia; [5]Department of Biomedical Sciences, Faculty of Medicine, Universitas Padjadjaran, Bandung, Jawa Barat, Indonesia; [6]School of Health Sciences, Universiti Sains Malaysia, Kota Bharu, KTN, Malaysia

*These authors contributed equally to this work

Correspondence: Kharisma Perdani Kusumahstuti, Doctoral Study Program, Faculty of Medicine, Universitas Padjadjaran, Bandung, Jawa Barat, 40125, Indonesia, Email kharisma.perdani@unpad.ac.id

Introduction: The most common cancer in women worldwide is breast cancer. Current systemic chemotherapies do not target specific cells, which makes them toxic to normal cells. The L-type amino acid transporter 1 (LAT1) is overexpressed in a lot of cancers, also in breast cancer. Few ligand such as JPH203 (KYT-0353), a known tyrosine analogue that specifically blocks LAT1, but have limitation. It has led to efforts to create next-generation LAT1 inhibitors or prodrugs with better qualities for target therapy or diagnostic.

Purpose: We investigated a new agent (S)-2-amino-4-(3,5-dichlorophenyl) butanoic acid (ADPB) as a new LAT1 inhibitor in three breast cancer cell lines: MCF-7 luminal A, HCC1954 HER2+, and MDA-MB-231 triple-negative. We hypothesized that the levels of LAT1 expression would influence the efficacy of ADPB. This could lead to a treatment that is more targeted and less harmful.

Methods: We used RT-qPCR to determine the LAT1 mRNA expression in each cell line and MTT for find IC_{50} values. These cells were given ADPB (0–160 μM) for 72 hours. There were three replication tests.

Results: ADPB diminished the viability of cells in all cell lines, and the effect was dose-dependent. MDA-MB-231 was the most sensitive cell line (IC_{50} = 118,1 μM 95% Cl (118,25–118,48), HCC-1954 was the middle-sensitive cell line (IC_{50} = 126,2 μM 95% Cl (126,11–126,68), and MCF-7 was the least sensitive cell line (IC_{50} = 127,3 μM 95% Cl (127,9–131,23). Study found an inverse relationship between LAT1 expression and IC_{50} in all cell lines, with higher LAT1 levels correlated with lower IC_{50}.

Conclusion: In this exploratory in vitro study, ADPB predominantly induces cytostatic effects, with cellular sensitivity associated with LAT1 expression in breast cancer cell line.

Keywords: LAT1, amino acid transporter, breast cancer, targeted therapy, cytostatic, theranostic agent

Introduction

Breast cancer is one of the most common types of cancer in woman worldwide. It was responsible for about 2.3 million new cases and 685,000 deaths in 2020 alone. It is the most common cancer in women and a significant cause of cancer deaths.[1] Breast cancer is one of the three most common types of cancer cause of cancer related death in Indonesia, along with lung and liver cancers.[2] These numbers show how important it is to come up with better ways to treat people, especially those with advanced disease who have the lowest chances of survival.

Based on receptor expression, breast tumours are different. They can be grouped into subtypes, such as luminal A/B (hormone receptor-positive), HER2-enriched, and basal-like/triple-negative (ER–/PR–/HER2).[3,4] Hormonal therapies

https://doi.org/10.2147/BCTT.S564513
Received: 1 September 2025
Accepted: 21 March 2026
Published: 7 May 2026

usually work on luminal subtypes (ER/PR-positive) and have better outcomes. On the other hand, HER2-positive and triple-negative breast cancers (TNBCs) are more aggressive and often do not respond to standard treatments. These aggressive subtypes are known to have higher metabolic activity and growth rates.[3,4] Traditional chemotherapies attack cells that are dividing quickly, but they do not choose which ones to attack, which causes severe damage to normal tissues like bone marrow and the lining of the stomach. There is a clear need for targeted therapies that take advantage of specific tumour characteristics to make them more effective and cause less harm to healthy cells.[5,6] One promising path is to focus on the metabolism of cancer cells, especially the nutrient transport systems that tumours need to keep growing. SLC7A5 encodes L-type amino acid transporter 1 (LAT1), which has become an interesting target in this situation.

People who have elevated LAT1 have been linked to more advanced disease and worse outcomes. These findings suggest that aggressive breast cancers become dependent on LAT1's amino acid influx, which helps them grow quickly and change their metabolism. LAT1 activity feeds the mTORC1 signalling pathway by giving it leucine and other important amino acids.[4,7] Importantly, targeting LAT1 may not have much of an effect on normal tissues because LAT1 is not very active in most adult normal cells. There are several LAT1 inhibitors in the works. The most advanced is JPH203 (KYT-0353), a tyrosine analogue that specifically blocks LAT1 without affecting other transporters.[8–10] However, limitations in solubility and pharmacokinetics have driven interest in alternative LAT1 targeting strategies. This gap has led to efforts to create next-generation LAT1 inhibitors or prodrugs with better qualities.[7,11,12]

We are looking at a new small-molecule LAT1 inhibitor candidate in this study. Its name is (S)-2-amino-4-(3,5-dichlorophenyl)butanoic acid or ADPB for short. We assessed ADPB in three breast cancer cell lines representing distinct molecular subtypes and expected differences in LAT1 expression. These cell lines are MCF-7 (luminal A, hormone receptor-positive), HCC1954 (HER2-overexpressing), and MDA-MB-231 (triple-negative). Prior evidence suggests that luminal models such as MCF-7 may exhibit lower LAT1 levels than more aggressive lines, including MDA-MB-231, with regulatory contributions from pathways such as the aryl hydrocarbon receptor.[6,8,13,14] We therefore hypothesised that ADPB sensitivity would relate to LAT1 expression, with greater growth inhibition in LAT1-high models. To our knowledge, ADPB has not been previously evaluated in breast cancer biological models.

The objective of this study was: (1) to measure LAT1 expression in the MCF-7, HCC1954, and MDA-MB-231 cell lines; (2) to test how well ADPB kills cells in these cell lines using MTT assays and find IC_{50} values; (3) to look at the link between LAT1 expression levels and ADPB sensitivity; and (4) to explore what kind of effect ADPB has on cell growth and what its possible benefits are (like being useful for theranostic use) and what this means for understanding how it works. This study is in line with the larger goal of precision oncology, which is to find treatments that target cancer-specific weaknesses while causing the least amount of damage to healthy tissues.[5,8,13] Our results will help initially determine if ADPB is a suitable candidate for further preclinical research as a LAT1-targeted breast cancer treatment.

Materials and Methods

Growth and Cell Lines

Three human breast cancer cell lines were used: MDA-MB-231 (triple-negative/basal-like), HCC1954 (HER2-positive), and MCF-7 (luminal A, ER/PR-positive, HER2-negative). These lines originated in the Laboratory of Cell Culture and Cytogenetics at the Faculty of Medicine Universitas Padjadjaran (Bandung, Indonesia). Ethical approval for the use of the cell lines was obtained from the Institutional Research Ethics Committee of Padjadjaran University, under approval number 609/UN6.KEP/EC/2025.

The cells were cultured in Gibco's RPMI-1640 medium supplemented with 10% heat-inactivated fetal bovine serum (FBS) and 1% penicillin-streptomycin. The cultures were maintained at 37°C in a humidified incubator with 5% CO_2. Every test was conducted in biological triplicate (three distinct cell culture experiments) using cells free of mycoplasma. Cells were used when they were 70–80% confluent and 10 passages from thaw to ensure consistency. Three wells were used for each treatment condition in each experiment to account for technical variations (Figure 1).

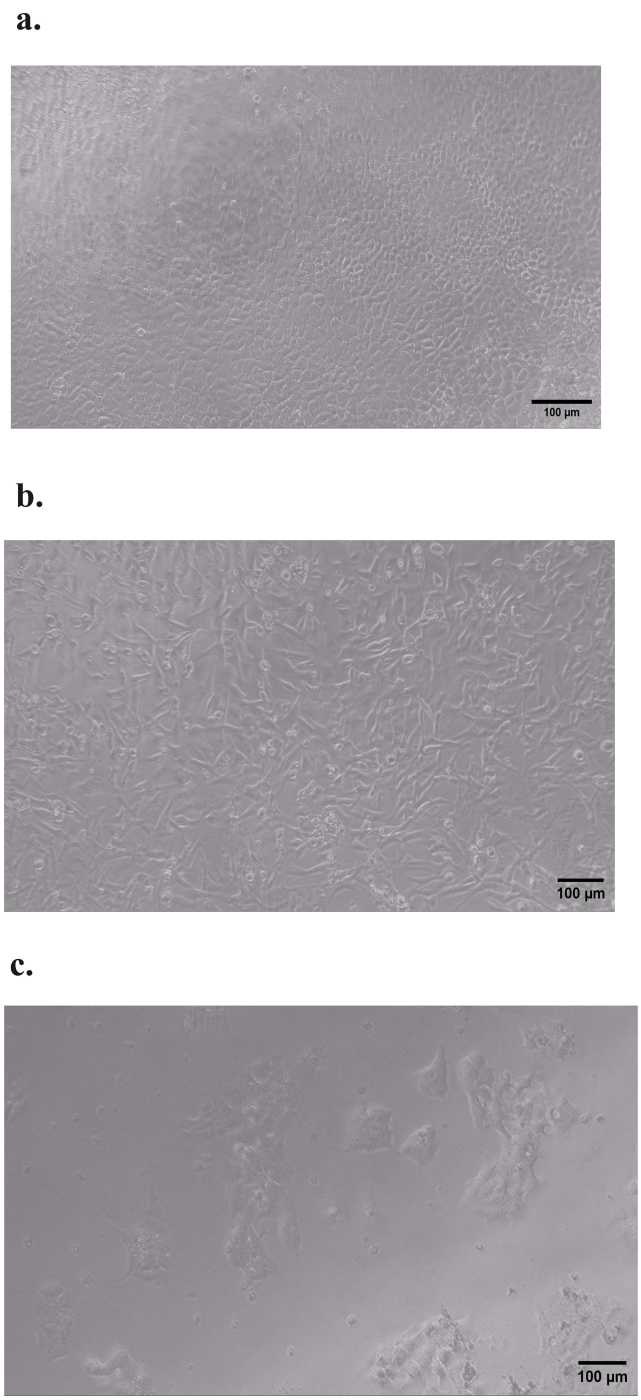

Figure 1 (**a**) MCF-7 cells (luminal A subtype) in monolayer culture, displaying epithelial clusters. (**b**) MDA-MB-231 cells (triple-negative subtype) with spindle-like morphology and a scattered growth pattern. (**c**) HCC1954 cells (HER2-positive subtype) show cohesive clusters with some epithelial morphology. Images were taken at 100× magnification prior to ADPB treatment.

Chemicals and Reagents

ADPB ((S)-2-amino-4-(3,5-dichlorophenyl)butanoic acid) was obtained from Amatek Chemical (purity >98% by HPLC). ADPB is a non-natural amino acid analogue with a molecular weight of 248.1 g/mol. It was stored as a powder at room temperature and dissolved in DMSO to create a 100 mM stock solution, which was aliquoted and kept at –20°C. Working concentrations were prepared freshly by diluting the stock in culture medium; the final DMSO concentration in medium

did not exceed 0.1% (vol/vol) in any treatment. For all experiments, control cells received an equivalent 0.1% DMSO vehicle.

Other reagents were of analytical grade. RPMI-1640 culture medium, FBS, and antibiotics were from Gibco/Thermo Fisher. The MTT reagent (3-(4,5-dimethylthiazol-2-yl)-2,5-diphenyltetrazolium bromide) and dimethyl sulfoxide (DMSO) were purchased from Merck. TRIzol reagent and a cDNA synthesis kit were from Invitrogen. The qPCR one-step kit (MyTaq One-Step RT-PCR) was from Bioline (BIO-72005). All buffer solutions and plasticware were sterile and nuclease-free where appropriate.

LAT1 Expression Analysis and RNA Extraction

Quantitative reverse transcription polymerase chain reaction (RT-qPCR) was implemented to evaluate LAT1 gene expression in each cell line. The cells were seeded in 6-well plates and cultivated until they reached approximately 80% confluence. Subsequently, they were extracted for RNA. The Quick-RNA™ Miniprep Plus reagent (Zymo Research, R1058) was employed to extract total RNA by the manufacturer's protocol. The RNA concentration and purity were assessed using spectrophotometry (NanoDrop 260/280 nm ratio; values between 1.8 and 2.0 were considered acceptable). The one-step RT-qPCR, which integrates reverse transcription and PCR in a single reaction tube, was performed using 1 μg of RNA as input for each sample. The Bioline MyTaq One-Step RT-PCR reagent was employed to establish the reactions on a Rotor-Gene Q real-time PCR cycler (Qiagen). Polymerase activation was conducted at 95°C for 2 minutes after reverse transcription was conducted at 45°C for 10 minutes. The cDNA was subsequently amplified through 40 cycles of PCR, which consisted of denaturation at 95°C for 5 s, annealing at 52°C for 10 s, and extension at 72°C for 5 s. The primer sequences for LAT1 (SLC7A5) were as follows: forward 5′-CATCGGGCTGTTACTGGCTC-3′ and reverse 5′-GCTGTAGCGATCCAGACACC -3′ (product ~150 bp). Primers were employed to quantify GAPDH mRNA as an internal control: forward 5′-TGCACCACCAACTGCTTAGC-3′ and reverse 5′-GGCATGGACTGTGGTCATGAG-3′ (product ~140 bp). Triplicate PCR wells were utilised to analyse each sample. To assess for contamination, a control without a template (water) was implemented.

The comparative Ct method (ΔΔCt) was employed to determine the relative expression of LAT1 in each cell line. MCF-7 was used as the calibrator (set as reference 1.0) and GAPDH as the housekeeping normaliser. Specifically, ΔCt = Ct LAT[1]– Ct^{GAPDH} for each sample, and ΔΔCt for HCC1954 or MDA-MB-231 = ΔCt(sample) – ΔCt(MCF-7). The relative mRNA level is calculated as 2 - $^{\Delta\Delta Ct}$ Livac method and Bashari et al.[15]

The results are presented as the fold-change in LAT1 expression in comparison to MCF-7.

Amplicon specificity was verified by melt-curve analysis (single peak consistent with a single product) and the expected amplicon size. The ΔΔCt method assumes comparable amplification efficiencies between target and reference assays; therefore, primer design was selected to yield similar efficiencies, and results should be interpreted with consideration of this assumption.

We also conducted each measurement in a minimum of three independent experiments to ensure that we had biological replicates.

Cell Viability (MTT) Assay and ADPB Treatment

The MTT assay was used to evaluate the anti-proliferative effect of ADPB, which measures metabolic activity (and, by extension, cell viability). To ensure that the control wells were 70–90% confluent at 72 hours, cells were plated in 96-well flat-bottom plates at an appropriate density (5×10^3 to 1×10^4 cells per well). Following 24 hours of cell attachment, cells were subjected to a variety of ADPB concentrations (0, 20, 40, 80, 160 μM). Five replicate wells were used to evaluate each concentration. The plates were incubated with ADPB for a continuous period of 72 hours. We selected a 72-hour exposure to ensure that ADPB could exert its anticipated cytostatic (rather than acutely cytotoxic) effect. The reference for 100% viability was untreated control wells (0 μM) with 0.1% DMSO.

After 72 hours, the viability of the cells was assessed by incubating each well at 37°C for 4 hours with 20 μL of MTT solution (5 mg/mL in PBS). MTT is converted to insoluble purple formazan crystals by metabolically active cells during this period. Then, 100 μL of DMSO was added to each well to dissolve the formazan, and the plates were gently agitated for 10 minutes. The Multiskan EX microplate reader (Thermo Fisher Scientific) was employed to measure the absorbance

at 550 nm. Background absorbance was subtracted from wells that contained media and MTT but did not contain cells. The viability of treated cells was quantified as a percentage of the control (0 μM ADPB) following normalisation.

For each cell line, we generated dose–response curves that plotted cell viability (%) against ADPB concentration. Figures 2a, 3a and 4a show the half-maximal inhibitory concentration (IC_{50}) was determined from these curves, which is the concentration of ADPB that reduces viability to 50% of the control (The IC_{50} values were determined by fitting a variable slope model with nonlinear regression). The viability curves for MCF-7, MDA-MB-231, and HCC1954, respectively, are depicted in Figures 2b, 3b, and 4b.

Qualitative morphological evaluations were implemented concurrently with MTT assays. Before MTT was added, cell monolayers were examined using an inverted microscope. This was done after the 72-hour treatment but before cell lysis occurs. This enabled the observation of cell confluence, shape, and evidence of cell mortality (eg., blebbing, floating cells) in each treatment condition. To document morphological changes, photomicrographs were acquired of representative fields for each cell line at the highest ADPB dose (160 μM). The images for MCF-7, MDA-MB-231, and HCC1954 are exhibited in Figures 2c, 3c, and 4c, respectively.

Lastly, in order to complement viability, which is indicative of both cell proliferation and death, we endeavoured to estimate the percentage of cells that had reduced at 72 hours by observing the fraction of cells that had lost adherence or exhibited membrane compromise. Although we did not conduct a designated live/dead staining or apoptosis assay, the reduction in confluence was employed as a proxy for cytostatic versus cytotoxic outcomes. We approximated the reduced cell percentage from the MTT data by presuming 100% viability, which represents the fraction of cells not metabolically active (including both dead and growth-arrested cells). This was done to gain a more quantitative understanding.

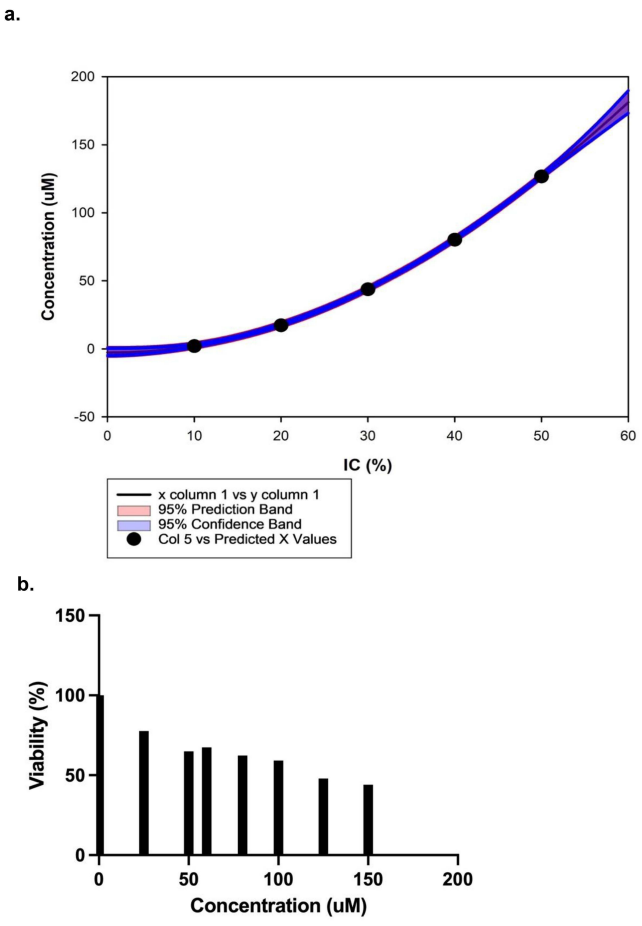

Figure 2 Continued.

https://doi.org/10.2147/BCTT.S564513

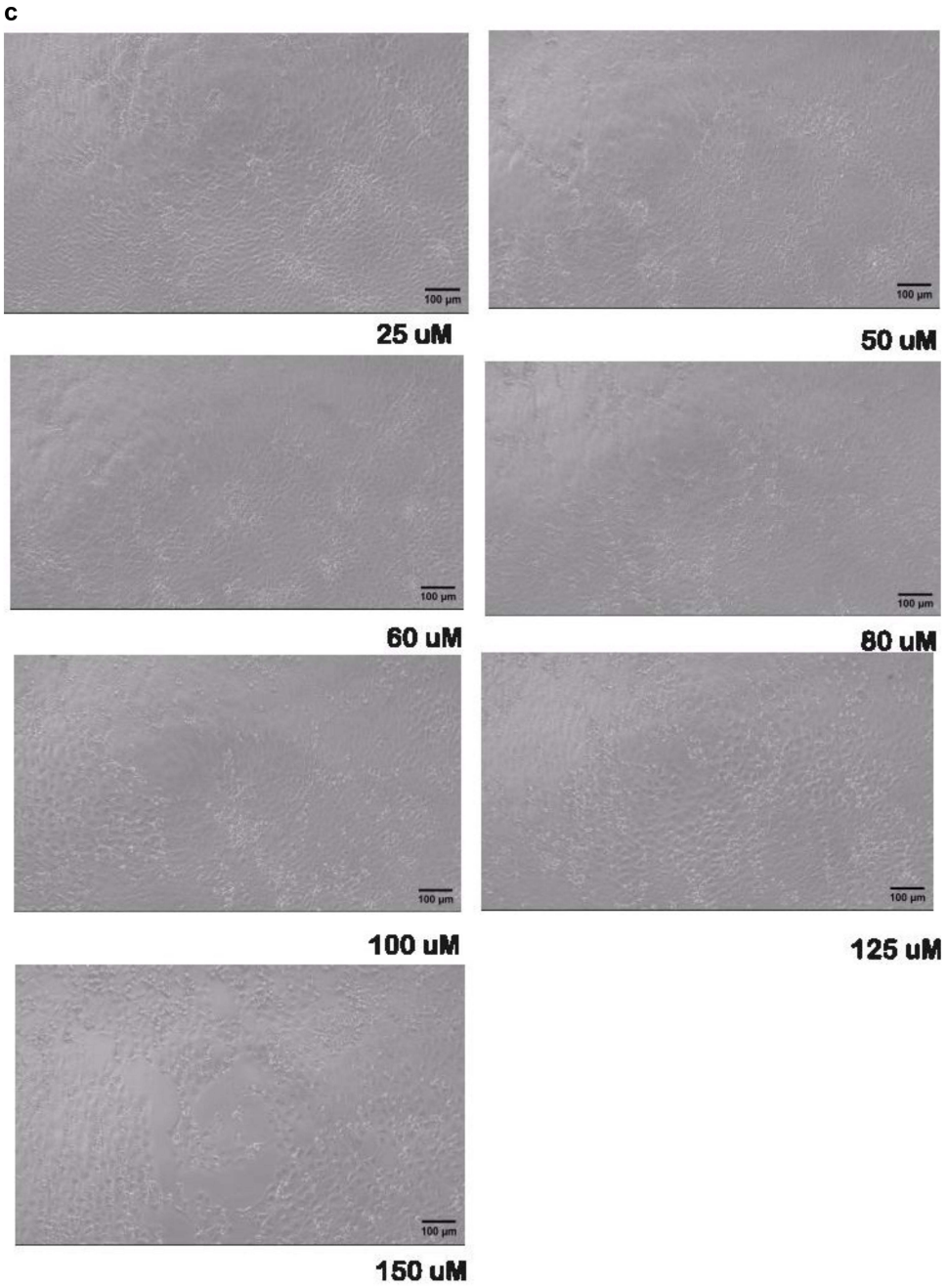

Figure 2 ADPB effects on MCF-7 cells (luminal A subtype, low LAT1). (a) Concentration–inhibition (IC) curve of ADPB in MCF-7 cells generated by nonlinear regression. The fitted curve is shown with the 95% confidence band (blue) and 95% prediction band (red), illustrating the precision of IC_{50} estimation in comparison with other IC levels (IC10–IC70). (b) MTT viability assay for MCF-7 after 72 h ADPB treatment. Cell viability declines with higher doses; IC_{50} =127.3 µM. Data are mean ± SD (n=3). (c) Phase-contrast images of MCF-7 cells under the microscope after treatment (representative field at 160 µM ADPB vs control). Treated cells show reduced confluence and slight rounding, but many cells remain attached without apoptotic morphology scale bar: 100 µm.

Additionally, we plotted these derived values against the dose. The decline in viability was consistent with the patterns of increasing viability reduced percentage with a higher ADPB dose.

Results are reported as viability (%) relative to vehicle-treated controls, calculated from absorbance values.

Protocol was register at: DOI: dx.doi.org/10.17504/protocols.io.36wgqpjr5vk5/v1

Analysis of Data

Unless otherwise indicated, all experiments were conducted in triplicate in independent trials. The data is presented as the mean ± standard deviation. One-way ANOVA followed by Dunett's multiple comparison test was employed to conduct statistical comparisons of LAT1 expression between cell lines with MCF-7 as control. Exact p-value is reported. For dose–response experiments, IC_{50} values were estimated by nonlinear regression using a four-parameter logistic (4PL; variable slope) model and are reported as IC_{50} with 95% confidence intervals together with goodness-of-fit metrics as provided by the regression output. The association between LAT1 expression and ADPB IC_{50} across the three cell lines (n = 3) is presented descriptively and no inferential claims or p-values are reported for this exploratory analysis.

All analyses and figure were performed using GraphPad Prism 10 and Sigma Plot 16. Figure images (microscopy and graphs) were assembled with labelling (a, b, c) and exported at 300–600 dpi resolution.

Each cell line's baseline shape and growth patterns were examined using an inverted phase-contrast microscope prior to treatment. Examples of microscopic images of the untreated cell lines are shown in Figure 1a: Clusters of polygonal cells adhered to one another as MCF-7 cells grew Figure 1b. MDA-MB-231 cells were dispersed and resembled spindles more. Figure 1c. HCC1954 cells produced cobblestone-like epithelial colonies.

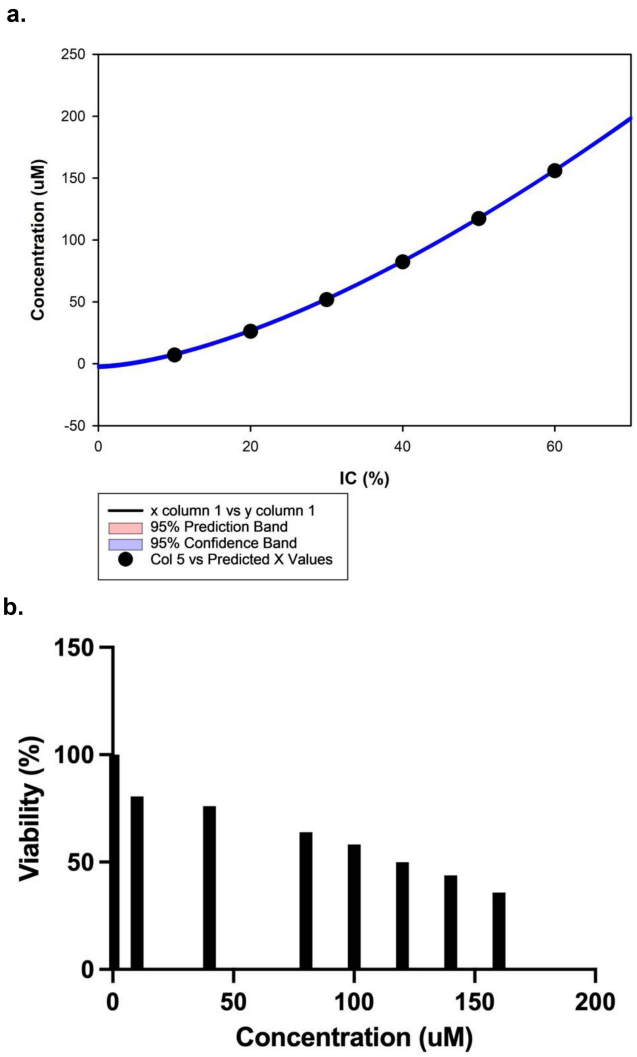

Figure 3 Continued.

https://doi.org/10.2147/BCTT.S564513

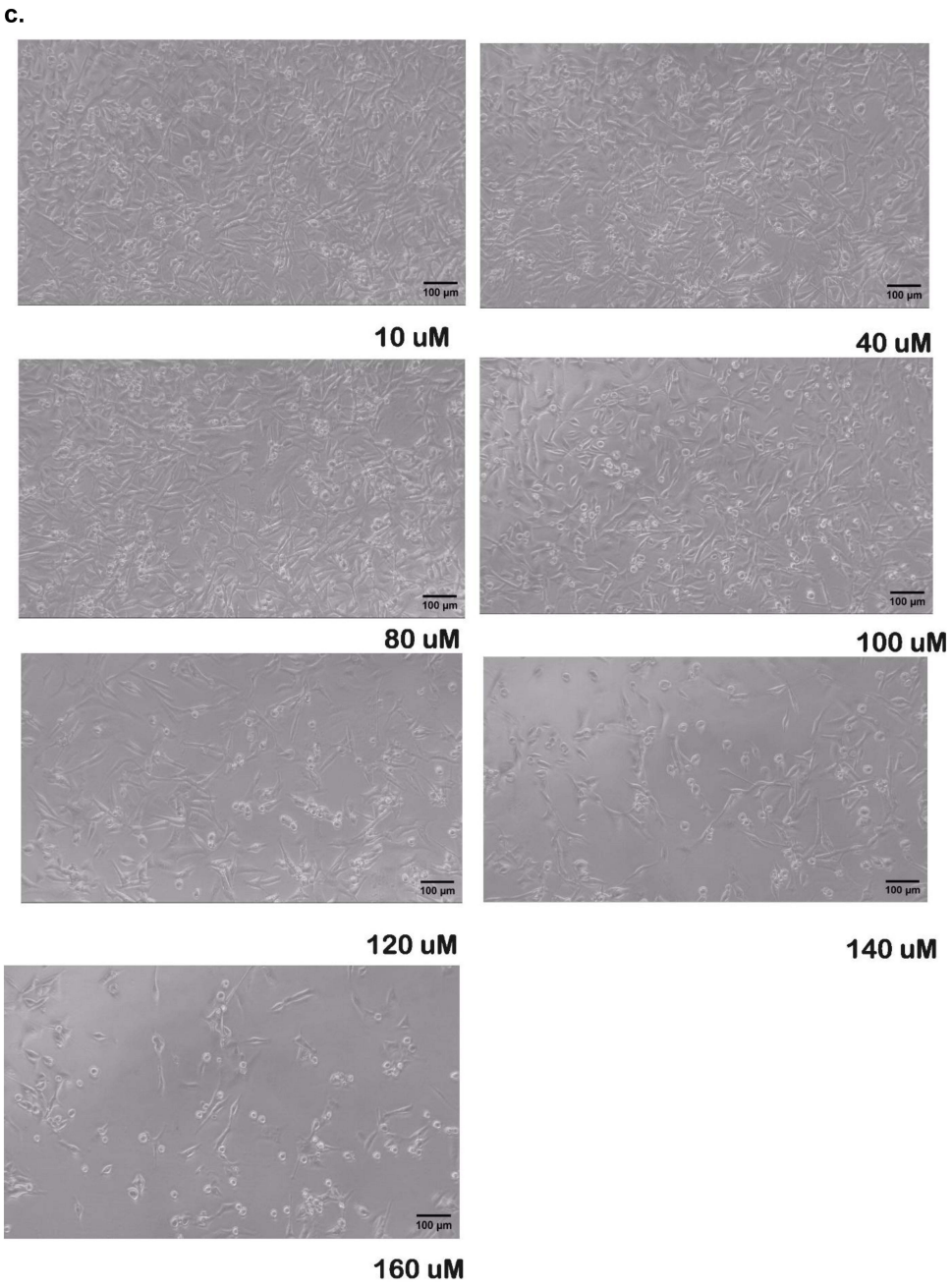

Figure 3 ADPB effects on MDA-MB-231 cells (triple-negative subtype, high LAT1). (a) Concentration–inhibition (IC) curve of ADPB in MDA-MB-231 cells generated by nonlinear regression. The fitted curve is shown with the 95% confidence band (blue) and 95% prediction band (red), illustrating the precision of IC_{50} estimation in comparison with other IC levels (IC10–IC70). (b) Cell viability curve (MTT assay) after 72 h treatment. MDA-MB-231 shows a steep drop in viability with increasing ADPB; IC_{50} =118.2 µM. Error bars = SD. (c) Microscopic images of MDA-MB-231 after treatment (160 µM vs control). High-dose ADPB caused most cells to round up and detach, drastically reducing the monolayer density. Only a few cells remained attached and viable.

Results

Each cell line's baseline shape and growth patterns were examined using an inverted phase-contrast microscope prior to treatment. Examples of microscopic images of the untreated cell lines are shown in Figure 1a: Clusters of polygonal cells adhered to one another as MCF-7 cells grew Figure 1b. MDA-MB-231 cells were dispersed and resembled spindles more. Figure 1c. HCC1954 cells produced cobblestone-like epithelial colonies.

Differential LAT1 Expression in Breast Cancer Cell Lines

Quantitative RT-PCR showed that the three breast cancer cell lines had very different levels of LAT1 mRNA expression (Figure 5). MDA-MB-231 cells had the most LAT1 expression, HCC1954 had a medium amount, and MCF-7 had the least. The relative SLC7A5 expression was about 35 times higher in MDA-MB-231 and 0.14 times (14%) higher in HCC1954, with MCF-7 as the reference (1.0-fold). LAT1 transcripts were challenging to find in MCF-7, but they were much higher in MDA-MB-231 ($p < 0.00159$s MCF-7), and HCC-1954 had intermediate but significantly higher levels than MCF-7 ($p < 0.0149$) (Figure 5).

The study found that LAT1 levels are higher in MDA-MB-231, which aids in leucine influx into cells for mTOR and protein synthesis. This excess may promote cell growth in nutrient-poor environments. HER2+ cells had more LAT1 than MCF-7, likely due to higher metabolic needs in these cancers.

Viability Cell of ADPB on MCF-7 Cells (Luminal A)

We first evaluated ADPB's effect on the MCF-7 cell line, which had the lowest LAT1 expression. MCF-7 cells were treated with increasing concentrations of ADPB (0–160 μM) for 72 h, and cell viability was measured by MTT assay. Figure 2a shows Concentration–inhibition (IC) curve of ADPB in MCF-7 cells generated by nonlinear regression. The fitted curve is shown with the 95% confidence band (blue) and 95% prediction band (red), illustrating the precision of IC_{50} estimation in comparison with other IC levels (IC_{10}–IC_{70}). Figure 2b shows the dose–response curve for MCF-7. ADPB caused a gradual, dose-dependent reduction in MCF-7 viability. At the lowest doses (20–40 μM), the effect was modest:

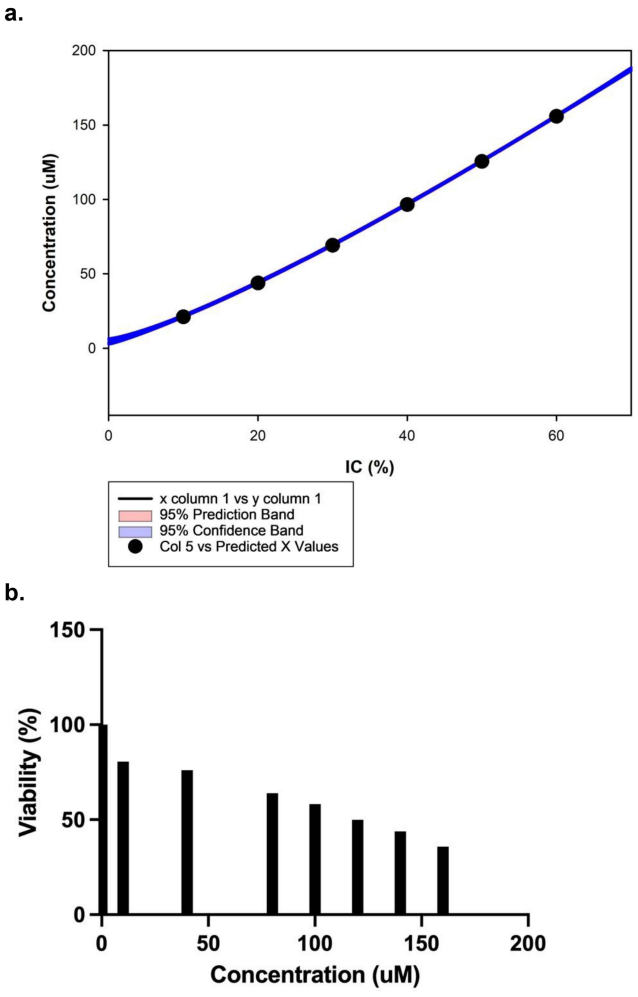

Figure 4 Continued.

https://doi.org/10.2147/BCTT.S564513

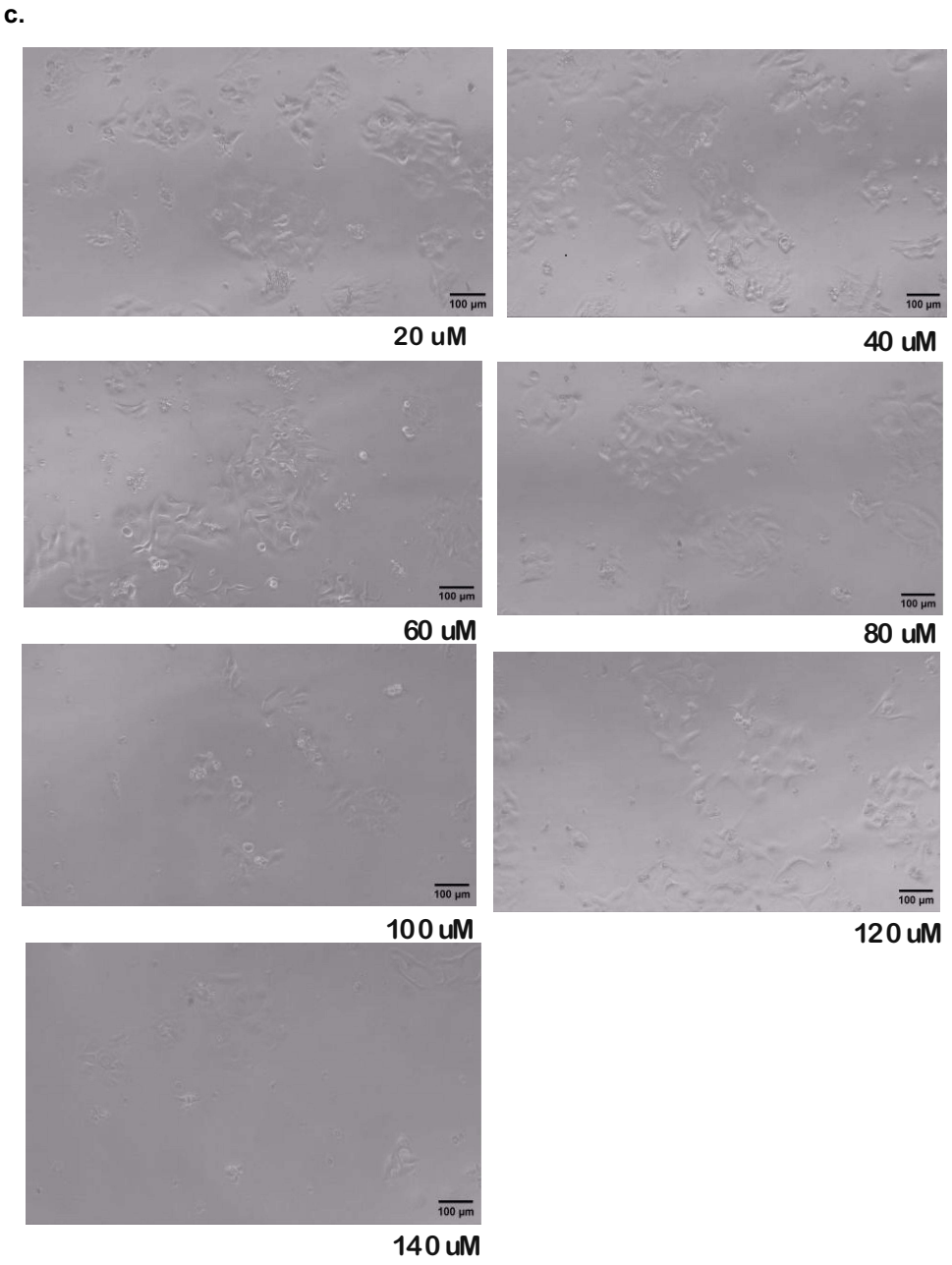

Figure 4 ADPB effects on HCC-1954 cells (HER2-positive subtype, moderate LAT1). (a) Concentration–inhibition (IC) curve of ADPB in HCC-1954 cells generated by nonlinear regression. The fitted curve is shown with the 95% confidence band (blue) and 95% prediction band (red), illustrating the precision of IC_{50} estimation in comparison with other IC levels (IC10–IC70). b) Viability curve after 72 h ADPB. HCC1954's IC_{50} =126.2 µM (very similar to MCF-7), reflecting moderate sensitivity. Error bars = SD. (c) Microscopy of HCC1954 post-ADPB (160 µM vs control). Treated cells show reduced cluster size and some cell detachment, but a notable fraction of cells remain attached and intact.

viability remained ~80–90% of control. As the dose increased to 80 µM and 160 µM, viability declined more substantially. We determined an IC_{50} (72 h) of 127.3 µM for ADPB in MCF-7 (95% CI 127,9–131,2 µM). The IC_{25} (concentration reducing viability by 25%) was approximately 30.0 µM (Figure 2a). These values indicate that MCF-7 cells are relatively less sensitive to ADPB, requiring over 100 µM to achieve 50% growth inhibition. For comparison, conventional chemotherapeutic drugs often have IC_{50} in low micromolar or nanomolar ranges in vitro; ADPB's higher IC_{50} suggests a moderate potency at best in this cell line.

Morphologically, untreated MCF-7 cultures formed a nearly confluent monolayer of adherent cells by 72 h. With ADPB treatment, we observed a dose-dependent decrease in cell density (confluence). At 160 µM, the MCF-7 monolayer

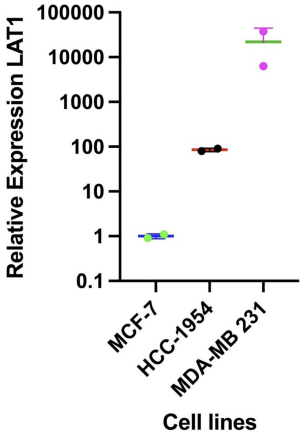

Figure 5 Relative expression levels in MCF-7, HCC-1954, and MDA-MB-231 cells displayed on a logarithmic scale (Y-axis is log10-scaled.). Data are presented as mean ± SD from n = 3 independent biological replicates; statistical significance was assessed by one-way ANOVA($p = 0.00223$) followed by Dunnett's multiple comparisons test versus MCF-7 (HCC-1954 vs MCF-7: $p = 0.0149$; MDA-MB-231 vs MCF-7: $p = 0.00159$). Error bars indicate SD (n=3).

was no longer confluent, some cells had detached or shrunk, and there were visible gaps between cell clusters (Figure 2c). However, even at the highest dose, a considerable proportion of MCF-7 cells remained attached and viable (many cells retained normal epithelial morphology, without overt signs of apoptosis such as membrane blebbing or fragmentation). This suggests that ADPB did not acutely kill the majority of MCF-7 cells but rather slowed their growth (cytostatic effect). Indeed, after 72 h at 160 μM, cell viability was still 40–50%, implying roughly half the cells survived or remained metabolically active.

To quantify cell reduced in MCF-7, we inferred that at 160 μM ADPB, 50–60% of cells were decreased or non-proliferating (since viability was 40–50%). For MCF-7, viability % rose gradually, reaching ~50–60% at 160 μM. The inflexion of the viability curve was shallow, reflecting MCF-7's relative resistance.

Phase-contrast images of MCF-7 cells under the microscope after treatment (representative field at 160 μM ADPB vs control). Treated cells show reduced confluence and slight rounding, but many cells remain attached without apoptotic morphology (Figure 2c).

Viability Cell of ADPB on MDA-MB-231 Cells (Triple-Negative)

We also examined MDA-MB-231, the triple-negative cell line with the highest LAT1 expression. ADPB produced a more pronounced effect in MDA-MB-231 than in MCF-7. Figure 3a shows Concentration–inhibition (IC) curve of ADPB in MDA-MB-231 cells generated by nonlinear regression. The fitted curve is shown with the 95% confidence band (blue) and 95% prediction band (red), illustrating the precision of IC_{50} estimation in comparison with other IC levels (IC_{10}–IC_{70}).

As shown in Figure 3b, cell viability dropped in a sharper dose-dependent manner. At 40 μM ADPB, MDA-MB-231 viability was reduced to (70% of control) and further declined to 50% at 80 μM. The IC_{50} for ADPB in MDA-MB-231 was calculated to be 118.2 μM (slightly lower than for MCF-7). The IC_{25} was 39.4 μM (Figure 3a). Notably, the MDA-MB-231 dose–response curve appears steeper: viability fell rapidly beyond 40–50 μM. By 160 μM, viability was only 20–30%, indicating a substantial loss of viable cells. This suggests that MDA-MB-231 cells are more sensitive to ADPB. The higher sensitivity correlates with their higher LAT1 levels, supporting our hypothesis of LAT1-mediated uptake or action of ADPB.

Morphological observations reinforce this. Untreated MDA-MB-231 cells grew as spindled, loosely attached cells. Upon ADPB exposure, especially at ≥80 μM, many MDA-MB-231 cells became rounded and detached from the plate (floating in the medium). At the top dose (160 μM), most cells were either dead or growth-arrested; only sparse viable cells remained adherent (Figure 3c). The treated cells did not show classic apoptotic blebbing, but widespread detachment suggests loss of viability. When replacing media after 72 h, many dead cells were visibly removed.

https://doi.org/10.2147/BCTT.S564513

At 160 μM, about 80% of the MDA-MB-231 cells were decreased (viability was about 20%). This means that ADPB had a stronger cytotoxic (or at least antiproliferative) effect on MDA-MB-231. The concentration-response profile shows that MDA-MB-231 cells cannot keep growing once they reach a certain level (about 50 μM). We think this might be because LAT1 takes up ADPB so well that it causes the cells to grow out of amino acids and stress responses (like the unfolded protein response) that MDA-MB-231 cannot fully contribute for.A study by Yamaga et al that is relevant found that TNBC cells like MDA-MB-231, when treated with a LAT1 inhibitor (JPH203), go through amino acid deprivation stress and may turn on antioxidant pathways to stay alive, but only for a short time.[16] Our results support the idea that MDA-MB-231's high LAT1 makes them depend on amino acid import and blocking it with ADPB makes them much less viable.

It is interesting to note that MDA-MB-231 was more affected by ADPB than MCF-7, but the absolute IC_{50} values are still relatively high for both (in the 100 μM range). This could mean that ADPB is not very strong, or that 72 hours were not enough time to see all of its cytotoxic effects (if ADPB mostly stops cells from dividing, cells might need more time to die). Also, MDA-MB-231's IC_{50} (118 μM) was only slightly lower than HCC1954's (as shown below), which suggests that other things besides LAT1 might affect sensitivity, like differences in metabolism or the cell cycle. Even so, the order of sensitivity from MDA-MB-231 to HCC1954 to MCF-7 is the same as the order of LAT1 expression.

Viability Cell of ADPB on HCC1954 Cells (HER2-Positive)

HCC1954 cells (HER2-enriched subtype) showed an intermediate response to ADPB. Figure 4a shows Concentration–inhibition (IC) curve of ADPB in HCC1954 cells generated by nonlinear regression. The fitted curve is shown with the 95% confidence band (blue) and 95% prediction band (red), illustrating the precision of IC_{50} estimation in comparison with other IC levels (IC_{10}–IC_{70}).

Figure 4b illustrates their viability dose–response. At low doses (20–40 μM), HCC1954 viability remained above 85%. A noticeable decline occurred at 80 μM (~65% viability), and at 160 μM, viability dropped to ~30%. The IC_{50} for HCC1954 was ~126.2 μM, very close to that of MCF-7 (127 μM) and slightly higher than MDA-MB-231. The IC_{25} was ~57.0 μM (Figure 4a). This places HCC1954's sensitivity between MCF-7 and MDA-MB-231, which is logical given HCC1954's LAT1 expression was also intermediate. However, interestingly, HCC1954's IC_{50} (~126 μM) was essentially the same as MCF-7's (~127 μM) within experimental error. This suggests that despite having higher LAT1 than MCF-7, HCC1954 did not respond more strongly to ADPB. One explanation could be that HCC1954, being HER2-driven, might rely less on amino acid uptake than the highly metabolic MDA-MB-231 (TNBC) cells, or it may have efficient compensatory pathways (eg., using alternate transporters or stored nutrients). Another reason might be experimental variability, our qPCR showed only a modest difference between HCC1954 and MCF-7 in LAT1 levels (MCF-7 was extremely low, and HCC1954 was low as well, albeit not as near-zero as MCF-7). Thus, both MCF-7 and HCC1954 may fall below a threshold of LAT1 expression needed for robust ADPB uptake and effect.

Microscopic observations of HCC1954 cultures treated with ADPB (Figure 4c) revealed dose-dependent changes similar to the other lines. Control HCC1954 cells grew as adherent clusters of polygonal cells. At high ADPB doses, cell density decreased, and some cells rounded up or detached. Compared to MDA-MB-231, HCC1954 had slightly better survival at 160 μM, patches of viable cells remained, although fewer than in MCF-7. There were no dramatic apoptotic figures but reduced cell-cell contact and some floating cells were noted. This again points to a partial cytostatic effect.

The estimated reduce viability cell percentage for HCC1954 (Figure 4b) droped with dose, reaching ~70% at 160 μM (viability ~30%). This is somewhat higher cell death than MCF-7 (~50%) but a bit lower than MDA-MB-231 (~80%). Thus, HCC1954's outcome was intermediate. We did not perform a statistical comparison of IC_{50} values between lines due to limited replicates, but qualitatively: MDA-MB-231 was the most susceptible to ADPB, and MCF-7 the least, with HCC1954 in between. These data support a trend of inverse relationship between LAT1 expression and ADPB IC_{50} (further quantified below).

Table 1 show summarizes the IC_{50} values of ADPB obtained by four-parameter logistic nonlinear regression.

Table 1 IC_{50} Summary (Nonlinear Regression) and Assay Conditions

Compound	Cell Line/Model	Assay Readout	Exposure Time (h)	Seeding Density (Cells/Well)	Plate Format	Vehicle (% v/v)	Dose Range (Units)	n (Biological)	n (Technical per Biological)	Model (4PL) Setting	IC_{50} (Units)	95% CI (Units)	Hill Slope	Goodness-of-Fit
ADPB	MCF-7	MTT (A570)	[72]	[1000]	96	[DMSO 0.1%]	[0–150] μM	[3]	[3]	Standar curve	[127,3]	[127,9–131,23]	[1,019]	R^2 = [1,000]
ADPB	HCC-1954	MTT (A570)	[72]	[1000]	96	[DMSO 0.1%]]	[0–160] μM	[3]	[3]	Standar curve	[126,2]	[126,11–126,68]	[1,56]	R^2 = [1,000]
ADPB	MDA-MB-231	MTT (A570)	[72]	[1000]	96	[DMSO 0.1%]]	[0–140] μM	[3]	[3]	Standar curve	[118,17]	[118,25–118,48]	[1.22]	R^2 = [1,000]

https://doi.org/10.2147/BCTT.S564513

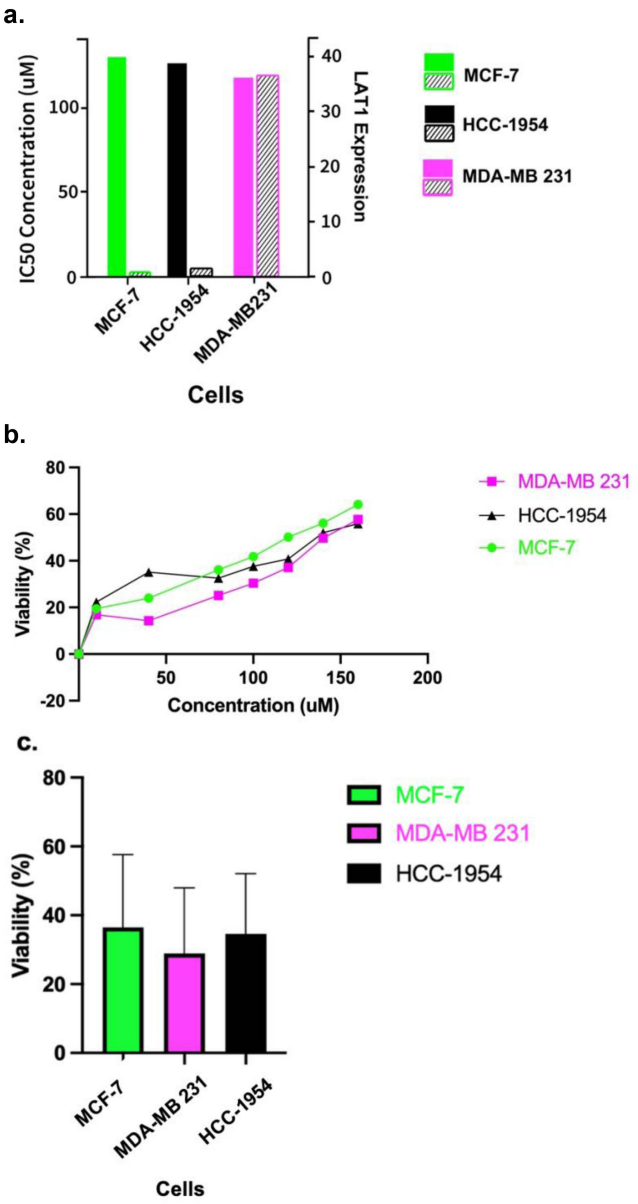

Figure 6 Relationship between LAT1 expression and ADPB response. (**a**) Correlation between LAT1 expression and ADPB IC_{50} across the three cell lines. Bars show IC_{50} values (left y-axis, in μM) for MCF-7 (green), HCC1954 (black), and MDA-MB-231 (pink). Overlaid diamonds show relative LAT1 mRNA expression (right y-axis). (**b**) Combined dose–response curves of ADPB treatment in MCF-7, HCC1954, and MDA-MB-231. Here, the outcome is plotted as % viability vs ADPB concentration, with each cell line indicated (green circles = MCF-7, black squares = HCC1954, pink triangles = MDA-MB-231). (**c**) Bars represent the percentage of viability after 72 h at 160 μM: Error bars = SD.

Relationship Between LAT1 Expression and ADPB Sensitivity

To directly examine the correlation between LAT1 levels and ADPB efficacy, we plotted the IC_{50} values of ADPB for each cell line against their relative LAT1 expression (Figure 6a). Despite having only three data points, an inverse correlation is apparent: MDA-MB-231, with the highest LAT1, had the lowest IC_{50} (~118 μM), whereas MCF-7, with negligible LAT1, had the highest IC_{50} (~127 μM), and HCC1954 fell in the middle (LAT1 moderate, IC_{50} ~126 μM). The association between LAT1 expression and ADPB IC_{50} across the three cell lines (n = 3) is presented descriptively, and no p-values are reported.

Figure 6b shows combined dose–response curves of ADPB treatment in MCF-7, HCC1954, and MDA-MB-231. Figure 6c shows bars viability % ADPB for each cell line against ADPB.

However, the trend points to an inverse relationship: greater ADPB sensitivity (lower IC_{50}) is associated with higher LAT1 expression, and vice versa. Practically speaking, this means that while LAT1 low expression may be more resistant to ADPB treatment, LAT1 high expression may respond better. As HER2 expression predicts response to anti-HER2 medications, LAT1 may therefore function as a predictive biomarker for ADPB efficacy. Our initial findings support the mechanistic hypothesis that ADPB acts as a putative LAT1 targeted agent and that its effects are LAT1 dependent.

Discussion

First, we looked at how ADPB affected the MCF-7 cell line, which had the lowest LAT1 expression. We treated MCF-7 cells with different amounts of ADPB (0–160 μM) for 72 hours and then used the MTT assay to check how many cells were still alive. The dose–response curve for MCF-7 is shown in Figure 2b. ADPB slowly and in a dose-dependent way killed MCF-7 cells. At the lowest doses (20–40 μM), the effect was small: viability stayed at about 80–90% of the control. As the dose increased to 80 μM and 160 μM, the viability decreased further. We found that the IC_{50} (72 h) for ADPB in MCF-7 was about 127.3 μM, with a 95% confidence interval of about 120–135 μM. The IC_{25} (the amount that makes cells less viable by 25%) was about 30.0 μM. These numbers show that MCF-7 cells are not very sensitive to ADPB; it takes more than 100 μM to stop their proliferation by 50%. In vitro, the IC_{50} of regular chemotherapy medicines is usually in the low micromolar or nanomolar range. ADPB's greater IC_{50} shows that it is only moderately potent in this cell line.

By 72 hours, untreated MCF-7 cultures had created a practically confluent monolayer of cells that stuck together. We saw that cell density (confluence) decreased after ADPB treatment in a dose-dependent way. At 160 μM, the MCF-7 monolayer was no longer confluent; some cells had come loose or shrank, and there were gaps between cell clusters (Figure 2c). However, even at the highest dose, a lot of MCF-7 cells stayed connected and alive (many cells kept their usual epithelial shape and did not show any obvious indicators of death, including membrane blebbing or disintegration). This means that ADPB did not kill most of the MCF-7 cells right away, but it did limit their development (cytostatic effect). After 72 hours at 160 μM, cell viability was still about 40–50%, which means that about half of the cells survived or stayed metabolically active.

To measure cell death in MCF-7, we estimated that approximately 50–60% of the cells were dead or non-proliferating at 160 μM ADPB, given a viability of about 40–50%. Figure 2a shows the estimated percentage of cell death in MCF-7 as a function of dosage. We figured this out by taking 100% and subtracting the viability. For MCF-7, the percentage of cell death slowly went up until it reached about 50–60% at 160 μM. The viability curve's inflexion was slight, which showed that MCF-7 was somewhat resistant. These results support the idea that LAT1 is more active in more aggressive phenotypes.[6]

Other studies have also found low LAT1 levels in hormone-responsive luminal cells and high LAT1 levels in basal/HER2+ cells.[6,8,13] In our tests, the expression values (adjusted for GAPDH) were as follows: MCF-7 is set to 1.0 (the baseline), HCC1954 is about 0.14, and MDA-MB-231 is about 35.3. When we calibrated HCC1954 to MCF-7, we found that HCC1954 had a very low relative value. This means that MCF-7 itself had very low LAT1 (close to the detection limit, or about 0 in arbitrary units), while HCC1954 was higher than MCF-7 but still a lot lower than MDA-MB-231. To sum up, MDA-MB-231 had the most LAT1 expression, followed by HCC1954 and MCF-7 (almost none). These differences made it easy to test if LAT1 levels affect how sensitive a cell is to ADPB. However, the data also highlight that ADPB's action is cytostatic rather than acutely cytotoxic, and that its potency in monotherapy is moderate (IC_{50} in the 100+ μM range).

We discuss below the implications of these results, the mechanistic considerations, and potential strategies to enhance ADPB's efficacy.

We first address the LAT1 expression patterns observed in our cell models, as this underpins ADPB's selective effect. We found MDA-MB-231 > HCC1954 > MCF-7 in terms of LAT1 mRNA levels, which aligns with the general expectation that more aggressive subtypes (triple-negative, HER2+) have higher LAT1 than the luminal subtype.[6] Clinical data support this trend. Shindo et al reported that LAT1 is upregulated in endocrine-resistant breast cancers and is associated with higher Ki-67 in luminal tumours.[17] Likewise, a recent review by Pae et al notes LAT1 is commonly elevated in aggressive cancers and has been proposed as a therapeutic target beyond breast cancer, eg., in

prostate and bladder cancers.[14,18] Our results are consistent with LAT1 being a marker of aggressive cancer cell metabolism.

Interestingly, some earlier studies had reported that MCF-7 can have substantial LAT1 expression under certain conditions. Tomblin et al showed that AHR knockdown reduced LAT1 in both MCF-7 and MDA-MB-231, implying that basal LAT1 is present and regulated by AHR in MCF-7 as well.[14] These reports might seem at odds with our data, where MCF-7 LAT1 was nearly undetectable A likely explanation is differences in experimental context that MCF-7 LAT1 expression can be influenced by culture conditions (eg., estrogen levels, cell density, or stress factors). In our experiments, MCF-7 cells were maintained in standard growth media without hormone deprivation. They might not strongly upregulate LAT1 unless subjected to metabolic stress. Other groups have indeed noted variability. Some have found MCF-7 expresses LAT1 protein moderately like study conducted by Liang et al, while others, like Yanagida et al, found higher LAT1 in MCF-7 than in specific other lines.[4,6] It is possible that technical differences (mRNA vs protein measurement, confluency, etc.) contribute to these discrepancies. Our data suggest that in our hands, MCF-7's LAT1 expression is minimal, reinforcing that it represents a LAT1-low, less metabolically aggressive phenotype compared to MDA-MB-231.

This discrepancy with some literature underscores a key point that LAT1 expression in breast cancer is not uniform and may be context dependent. Tumour heterogeneity means that some ER+ luminal tumours (or cell lines) could still have relatively high LAT1 if they have acquired aggressive features or in response to certain stimuli.[8,13] Conversely, some triple-negative models might not universally express LAT1 at the highest levels if alternate metabolic pathways are used. Our study's focus on three cell lines provides a snapshot, but a broader panel would be helpful to confirm the correlation. Nonetheless, the trend we observed supports the rationale of LAT1 as a therapeutic target and biomarker. Tumours with high LAT1 are likely those with high metabolic demands and possibly more malignant behaviour, making them suitable for LAT1-targeted interventions.[6]

ADPB was conceptualised as an alternative to JPH203, aiming to overcome some of JPH203's limitations while retaining LAT1 affinity. Our results show that ADPB does affect cell viability, which implies it reaches the intracellular target and perturbs cancer cell metabolism. The dependence of its effect on LAT1 levels suggests that ADPB likely enters cells via LAT1 or at least exerts its action in a LAT1-related manner (for instance, by competing with leucine at LAT1's binding site, thereby starving the cell). This is further supported by the observation that ADPB's pattern of activity mirrors that of leucine deprivation. It caused growth inhibition and only gradual cell death, similar to how leucine starvation triggers cell cycle arrest and autophagy rather than immediate apoptosis.[19]

Implications for LAT1 targeted therapy in breast cancer can be found in our study's findings. The concept that LAT1 is a viable target in breast cancer, particularly for aggressive subtypes. Although LAT1 inhibitors alone may not cause massive tumour cell kill, they can significantly suppress tumour growth. In a clinical context, a cytostatic agent can transform cancer into a more manageable chronic condition, especially if it prevents progression. For instance, an LAT1 inhibitor could slow tumour growth and metastasis, giving other treatments or the immune system. It will take more time to act. Moreover, LAT1 expression could be used to select patients likely to benefit. This is analogous to how we use ER, PR, and HER2 status; in the future, LAT1 immunohistochemistry on tumour biopsies might identify candidates for LAT1-targeted therapies. Zhou et al suggested LAT1 could serve as both a diagnostic and therapeutic target in breast cancer, and our findings support that notion that LAT1 high cells expression responded best to ADPB.[8,13]

One exciting avenue is the integration of LAT1 targeting in theranostics. With ADPB's apparent selectivity for LAT1-high cells, a radiolabeled form could be used for PET imaging to non-invasively gauge LAT1 expression in tumours. It is similar to how ^{18}F-FDG PET gauges glucose metabolism. LAT1 PET tracers like ^{18}F-FDOPA, ^{18}F-FAMT, have been explored for some cancers.[20] A successful LAT1 PET imaging could guide therapy. Patients with LAT1-positive tumours (hot uptake) might then receive a therapeutic isotope attached to the same compound. This is already done in neuroendocrine tumours with SSA receptor imaging & therapy, and in prostate cancer in PSMA-targeted theranostics. Given that LAT1 is expressed in many cancers including those with few other targets, like TNBC or certain sarcomas. A LAT1 theranostic could have a broad impact. Achmad et al highlight LAT1 as a potential pan-cancer target, meaning a single LAT1 directed agent could be repurposed for multiple tumour types that share this metabolic trait.[5]

For clinical synergy, we suggest that determining which current treatments LAT1 inhibitors work in concert with will be essential. In xenograft models, ADPB could be tested in conjunction with chemotherapy such as doxorubicin or

carboplatin for TNBC. Synergy might be seen if ADPB enforced nutrient deprivation increases tumour cells' chemo-sensitivity less ATP for drug efflux pumps. By transforming an efflux pump inhibitor into a LAT1-targeted form, Huttunen et al demonstrated a proof-of-concept that enhanced vinblastine accumulation and effectiveness in cancer cells. Montaser et al demonstrated that prodrugs that used LAT1 enhanced vinblastine uptake in the brain and increased apoptosis in cancer cells.[21,22] According to these studies, LAT1 targeting may improve the effectiveness or delivery of additional anticancer drugs. ADPB may also function as a sensitiser or carrier. LAT1-targeted cytotoxic can conjugate that selectively releases a toxin inside LAT1, expressing cells could be created by attaching a cytotoxic warhead to ADPB. This method uses a small molecule transporter targeting moiety and is comparable to antibody drug conjugates.

Limitation

While our study provides valuable insights, it has several limitations that must be acknowledged. The study evaluated three cell lines, one of which was breast cancer, to find the LAT1 connection. However, the conclusions about ADPB's mechanism would be stronger if they were based on more lines or primary patient cells. The study also did not conduct a direct LAT1 activity experiment, which would have demonstrated that ADPB inhibits LAT1 activity. The lack of apoptosis and cell cycle data also limited the study's understanding. The study only used in vitro tests, which could affect how well ADPB works in vivo things. The study did not investigate whether ADPB can penetrate 3D tumour designs or impact cell movement and invasion. The study did not examine the stability of ADPB in culture, which could impact its effectiveness. We thought that ADPB mostly worked through LAT1, but we did not rule out other targets or impacts that were not supposed to happen. The study used micromolar units to show concentrations, although the highest dose was 160 μM because the molecule cannot dissolve in water. Future studies should include a larger group of subjects and possibly LAT1 knockdown or overexpression trials to demonstrate that one thing causes another directly.

Despite these limitations, our results give us a starting point for further study on targeting ADPB and LAT1. These confirm that LAT1 is a legitimate target in our models and raise several follow-up issues, such as: Does ADPB, paired with an autophagy inhibitor, cause these cells to die? Can a radioisotope-labelled ADPB show LAT1-positive tumours? Do ADPB and regular chemotherapy work better together? We plan to look into these questions in more studies in the future. Based on what we have said so far, our work adds to the expansion of research that looks at metabolic weaknesses in cancer. Most traditional treatments focus on DNA or signalling proteins. Targeting nutrition availability through transporters like LAT1 is a newer idea. The idea is similar to cutting off the supply lines of a tumour. This method may not immediately eliminate the target (tumour), but it can significantly weaken it, making it easier to treat with other therapy or maintain control over its growth.

Conclusion

This exploratory in vitro study demonstrates that ADPB predominantly induces cytostatic effects, with cellular sensitivity associated with LAT1 expression in breast cancer cell line. Our result providing preliminary evidence that supports further mechanistic studies and orthogonal validation prior to consideration of therapeutic relevance in breast cancer. It will offer potential candidate for therapeutic selectivity and integrating ADPB into combination regimens to improve outcomes in hard-to-treat subtypes like TNBC and HER2-positive cancers in breast.

Abbreviations

ADPB, (S)-2-amino-4-(3,5-dichlorophenyl) butanoic acid; LAT1, L-type amino acid transporter 1; JPH203, Nanvuranlat, mRNA; messenger Ribonucleic Acid; MCF-7, Michigan Cancer Foundation; HCC1954-HER2, Human Epidermal Growth Factor Receptor-2; MDA-MD231, MD Anderson Metastatic Breast-231.

Acknowledgments

We thank Tenny Putri, Nurul, Ervi Afifah, Redi Regia Pratama, Fajar and Atikah Hana for technical support. The publication charge was supported by Universitas Padjadjaran (UNPAD) through the Indonesian Endowment Fund for Education (LPDP) under the Ministry of Higher Education, Science and Technology, as part of the EQUITY Program (Contract Nos. 4303/B3/DT.03.08/2025 and 3927/UN6.RKT/HK.07.00/2025).

Disclosure

The authors declare no conflicts of interest in this work.

References

1. Arnold M, Morgan E, Rumgay H, et al. Current and future burden of breast cancer: global statistics for 2020 and 2040. *Breast*. 2022;66:15–23. doi:10.1016/j.breast.2022.08.010
2. International Agency for Research on Cancer. *B). Global Cancer Observatory Fact Sheet: Indonesia*. World Health Organization; 2022. Available from: https://gco.iarc.who.int/media/globocan/factsheets/populations/360-indonesia-fact-sheet.pdf. Accessed March 30, 2026.
3. Elliyanti A, Hafizhah N, Salsabila D, et al. Exploring the promising therapeutic benefits of iodine and radioiodine in breast cancer cell lines. *Narra J*. 2024;4(3):e1078. doi:10.52225/narra.v4i3.1078
4. Yanagida O, Kanai Y, Chairoungdua A, et al. Human L-type amino acid transporter 1 (LAT1): characterization of function and expression in tumor cell lines. *Biochim Biophys Acta BBA - Biomembr*. 2001;1514(2):291–302. doi:10.1016/s0005-2736(01)00384-4
5. Achmad A, Lestari S, Holik HA, et al. Highly specific L-Type amino acid transporter 1 inhibition by JPH203 as a potential pan-cancer treatment. *Processes*. 2021;9(7):1170. doi:10.3390/pr9071170
6. Liang Z, Cho HT, Williams L, et al. Potential biomarker of L-type amino acid transporter 1 in breast cancer progression. *Nuclear Med Mol Imag*. 2011;45(2):93–102. doi:10.1007/s13139-010-0068-2
7. Kandasamy P, Gyimesi G, Kanai Y, Hediger MA. Amino acid transporters revisited: new views in health and disease. *Trends Biochem Sci*. 2018;43(10):752–789. doi:10.1016/j.tibs.2018.05.003
8. Zhao Y, Pu C, Liu K, Liu Z. Targeting LAT1 with JPH203 to reduce TNBC proliferation and reshape suppressive immune microenvironment by blocking essential amino acid uptake. *Amino Acids*. 2025;57(1):45. doi:10.1007/s00726-025-03456-3
9. Okano N, Hana K, Naruge D, et al. Biomarker analyses in patients with advanced solid tumors treated with the LAT1 inhibitor JPH203. *vivo*. 2020;34(5):2595–2606. doi:10.21873/invivo.12077
10. Wempe MF, Rice PJ, Lightner JW, et al. Metabolism and pharmacokinetic studies of JPH203, an L-Amino acid transporter 1 (LAT1) selective compound. *Drug Metab Pharmacokinet*. 2012;27(1):155–161. doi:10.2133/dmpk.DMPK-11-RG-091
11. Yan R, Zhao X, Lei J, Zhou Q. Structure of the human LAT1–4F2hc heteromeric amino acid transporter complex. *Nature*. 2019;568(7750):7750):127–130. doi:10.1038/s41586-019-1011-z
12. Häfliger P, Graff J, Rubin M, et al. The LAT1 inhibitor JPH203 reduces growth of thyroid carcinoma in a fully immunocompetent mouse model. *J Exp Clin Cancer Res*. 2018;37(1). doi:10.1186/s13046-018-0907-
13. Zhou Z, Zhu T, Zheng W, et al. LAT1 transporter as a target for breast cancer diagnosis and therapy. *European Journal of Medicinal Chemistry*. 2025;283:117064. doi:10.1016/j.ejmech.2024.117064
14. Tomblin JK, Arthur S, Primerano DA, et al. Aryl hydrocarbon receptor (AHR) regulation of L-Type Amino Acid Transporter 1 (LAT1) expression in MCF-7 and MDA-MB-231 breast cancer cells. *Biochemical Pharmacology*. 2016;106:94–103. doi:10.1016/j.bcp.2016.02.020
15. Bashari MH, Agung MUK, Ariyanto EF, et al. Two novel compounds isolated from the marine fungal symbiont of aspergillus unguis induce apoptosis and cell cycle arrest in breast cancer cells: in vitro study. *J Exp Pharmacol*. 2025;17:37–50. doi:10.2147/JEP.S494777
16. Yamaga T, Suehiro J, Wada Y, Sakurai H. Induction of CTH expression in response to amino acid starvation confers resistance to Anti-Lat1 therapy in MDA-MB-231 cells. *Sci Rep*. 2022;12(1). doi:10.1038/s41598-022-04987-5
17. Shindo H, Harada-Shoji N, Ebata A, et al. Targeting amino acid metabolic reprogramming via L- type amino acid transporter 1 (LAT1) for endocrine-resistant breast cancer. *Cancers*. 2021;13(17):4375. doi:10.3390/cancers13174375
18. Pae S, Sakamoto S, Zhao X, et al. Targeting L-type amino acid transporter 1 in urological malignancy: current status and future perspective. *J Pharmacol Sci*. 2022;150(4):251–258. doi:10.1016/j.jphs.2022.10.002
19. Fukui T, Yabumoto M, Nishida M, et al. Amino acid deprivation in cancer cells with compensatory autophagy induction increases sensitivity to autophagy inhibitors. *Mol Cell Oncol*. 2024;11(1). doi:10.1080/23723556.2024.2377404
20. Krämer SD, Mu L, Müller A, et al. 5-(2-^{18}F-fluoroethoxy)-L-tryptophan as a substrate of system L transport for tumor imaging by PET. *J Nuclear Med*. 2012;53(3):434–442. doi:10.2967/jnumed.111.096289
21. Huttunen J, Gynther M, Huttunen KM. Targeted efflux transporter inhibitors – a solution to improve poor cellular accumulation of anti-cancer agents. *Int J Pharmaceut*. 2018;550(1–2):278–289. doi:10.1016/j.ijpharm.2018.08.047
22. Montaser A, Markowicz-Piasecka M, Sikora J, Jalkanen A, Huttunen KM. L- type amino acid transporter 1 (LAT1)-utilizing efflux transporter inhibitors can improve the brain uptake and apoptosis-inducing effects of vinblastine in cancer cells. *Int J Pharmaceut*. 2020;586:119585. doi:10.1016/j.ijpharm.2020.119585